AN ANALYTIC STUDY OF THE PREDICTABILITY OF THE FLOW IN A DISH-PAN MODEL OF THE ATMOSPHERE

by

DOUGLAS WILLIAM DOCKERY

B.S., University of Maryland (1969)

SUBMITTED IN PARTIAL FULFILLMENT OF THE REQUIREMENTS FOR THE DEGREE OF MASTER OF SCIENCE

at the

MASSACHUSETTS INSTITUTE OF TECHNOLOGY

August, 1972

Signature of Author .....
Department of Meteorology, 14 August, 1972

Certified by .....
Thesis Supervisor

Accepted by .....
Chairman, Departmental Committee on Graduate Students

AN ANALYTIC STUDY OF THE PREDICTABILITY OF THE FLOW IN A DISH-PAN MODEL OF THE ATMOSPHERE

Douglas William Dockery

Submitted to the Department of Meteorology on 14 August 1972 in partial fulfillment of the requirements for the degree of Master of Science.

ABSTRACT

The growth of errors in a dish-pan model of the atmosphere was studied by means of analogues. Two states which resemble each other closely are termed analogues. Either state may be regarded as being equal to the other plus a small error. The rate of growth of this error may be determined by the subsequent behavior of the states.

One hundred streak photographs of the free surface velocity field were analyzed and fitted by least-squares to a truncated Fourier-Bessel series. The root-mean-square difference between the series representations was used as the difference between states, or the error.

An attempt was made to effectively increase the number of pairs by rotating the frame of reference of photographs and then computing the error. This procedure was not successful in increasing the number of "good" analogues and was not pursued.

There were numerous mediocre analogues but no truly good ones. The smallest errors encountered had an initial doubling time of 6.6 "days". Extrapolation with the aid of a quadratic hypothesis indicated that small errors would double in 1.7 "days". This is not statistically different from the doubling time of 2.5 "days" found similarly in studies of the atmosphere.

Thesis Supervisor: Edward N. Lorenz

Title: Professor of Meteorology

TABLE OF CONTENTS

1. INTRODUCTION

The reliability of weather forecasts has increased significantly during the past twenty years. In large part, this has been due to the application of digital computers in producing aids for the forecaster. The primary success has been in the prediction of the location and intensity of systems such as extratropical cyclones a day or two in advance. This success has fallen off sharply for longer prediction periods. Qualitatively the reasons for this decay of predictability with time are easily understood.

The atmosphere can be described by a system of dynamic equations. The forecasting process is an attempt to find a solution to that system of equations. The success we have had in forecasting has been primarily by techniques which extrapolate the current observed state of the atmosphere to find future states. Errors are introduced into such a forecast at the outset by our inability to observe the state of the atmosphere exactly at any time. We are limited in our observations to a discrete set of measuring sites which make up our observation network. The dynamics of the atmosphere on the other hand, are characterized by a continuous spectrum of scales. By measuring with a discrete observation network, we find the sub-grid scale energy appearing under an alias as energy of the large scale flow. This is an observational error in addition to the actual error in measurement. In order to eliminate this error in initial conditions, it would be necessary to measure the motions of the atmosphere down to the scale of the viscous dissipations - an impossible task. The success of the current short-range prediction

schemes is due to our ability to filter out these observational errors by "analysis" of the data. For longer prediction intervals, the errors produced by the extrapolation techniques themselves become dominant. Essentially a 48 hour forecast is a 24 hour forecast using as its initial state a previous 24 hour forecast. Likewise for 72 hours and so on. Thus, even assuming that the initial state of the atmosphere is perfectly known, the inaccuracies of the forecasting technique produce errors in the predictions which are used as initial conditions for further forecasts. Lorenz (1963) has demonstrated that the atmosphere is an unstable system such that the initial errors will grow until they are the size of the errors for randomly chosen initial conditions.

In as much as perfect forecasting of the weather is not possible, we would like to know how far in advance we can reliably predict. To date most of this quantitative work has been done by determining and comparing solutions of systems of dynamic equations which have characteristics similar to those of the atmosphere. Thompson (1957) considered a quasi-geostrophic model and concluded that errors in the initial data limited useful prediction to one week. Charney et al. (1966) considered the growth of errors in several primitive equation models of the general circulation, concluding that the limit of predictability in the atmosphere was two weeks. Lorenz (1969a) studied the predictability of various scales of motion using a barotropic model. He showed the doubling time of errors in the model to be a function of the scale of the motion in which the error is imbedded. Thus for example, errors in the specification of thunderstorms double in minutes while errors in the

specification of extra-tropical cyclones double in days. Note however that errors below the scale of our observation network are already as large as random errors. The appropriate errors to consider are those corresponding to the scale of the grid. Flemming (1971) has extended this work by applying stochastic dynamic methods to Lorenz' 28 variable model. Recently Leith (1971) has considered the growth of errors in a model of two-dimensional turbulence. Lorenz (1972) has studied analytically the growth of errors in a barotropic model of the atmosphere.

This study of mathematical models of the atmosphere is not completely satisfactory for there is the feeling, as Robinson (1967) points out, that they tell more about the predictability of the model than about the real atmosphere. Such models are based on approximations to the true governing equations of the atmosphere. In general they deal explicitly with only the larger scales of motions. It is not certain whether the effects of smaller scale motions are adequately represented. In particular, we have to question whether such models can adequately describe the influence of errors in the small scales of motion on the larger scales. As an alternative to the numerical modelling approach, Lorenz (1969) analyzed the growth of errors based upon actual atmospheric data. In principle, if we wait long enough we would expect to encounter a state which closely resembles some previous state, an analogue. Either state may be treated as equivalent to the other plus a small error. The growth of this error can then be studied by the subsequent behavior of the pair.

In his study of the atmosphere Lorenz considered five years of atmospheric data at three pressure levels for the years 1963-1967. States of the atmosphere within one month of each other, but in a different year, were compared. A total of over 400,000 pairs of states were considered. No truly good analogues were found. The smallest error encountered was more than half as great as the average error in the sample. The smallest errors encountered amplified by nearly ten percent per day which implies that small errors double in not more than eight days. From the distribution of the data it was estimated that it would require 140 years of data to find an error only half as large as the average.

Our current record of atmospheric observations up to only 500 mb extends back little more than twenty five years. Therefore, the additional information to be gained by studying the complete record of these observations seems small. However, because of the uniqueness of this approach in treating a real fluid system, including the influences of the smallest scales of motion, a study of the possibility of finding analogues in a laboratory model of the atmosphere was undertaken. Of course the objection that any conclusions we could draw from such a study are more applicable to the model than to the real atmosphere is equally valid as with the case of numerical models. However, we felt that this approach potentially would yield results not obtainable by numerical methods.

The laboratory model which most closely duplicates the atmosphere is the dish-pan experiment. Essentially it consists of a cylindrical

container, usually containing water, which is mounted on a rotating turntable. A heat source is provided at the rim with a cold source at the center. Although flows qualitatively similar to those of the atmosphere are easily obtained, quantitative investigations require extreme care (see Fultz et al. 1959). The flow in the dish-pan is known to be governed by equations very similar to those of the atmosphere. Here lies one significant difference between laboratory and numerical modelling. The dish-pan experiment is governed by equations of exactly the same form as those of the atmosphere. Thus the statistics of the dish-pan will reflect the influence of the sub-grid scales better than those of a numerical approximation of these equations. On the other hand, certain simplifications are made which differentiate the dish-pan from the atmosphere. The condensation of water vapor is not modelled in any way. Although there are indications of its importance in the tropics, from empirical studies in the dish-pan, it appears to be a minor influence in mid-latitudes. Because we are considering a cylindrical rather than spherical container, the β-effect, i.e. the tendency for relative vorticity to decrease in northward flow and increase in southward flow because of the variation of the Coriolis parameter, is not modelled. Although the β-effect is required for realistic results in numerical models, empirical studies in the dish-pan show it is not required for the development of flows similar to those of the atmosphere. Finally, the dish-pan is free of topography. As we shall see, this symmetry was an important consideration in the selection of this model.

Fultz et al. (1959) have studied the character of the flow in the dish-pan in detail. They found two qualitatively different regimes of flow, a zonally symmetric flow type known as the Hadley régime and a zonally asymmetric flow type known as the Rossby régime. The transition between these régimes is governed by the externally adjustable parameters of the experiment - the depth of the working fluid, the rotation rate, and the temperature contrast between the hot and cold sources. The Hadley type flow develops over a considerable range of these parameters and is characterized by an apparently perfectly symmetric flow about the axis of rotation. Under other conditions, however, the Rossby type flow develops. It is characterized by a strong "circumpolar" jet about the axis of rotation with wave-like disturbances superposed. The motion, like that of the atmosphere, is aperiodic. The free surface flow is very similar to that near the tropopause in the atmosphere. Furthermore, Faller (1956) has demonstrated, by placing dye crystals at the bottom of the pan, the existence of fronts and migratory cyclones whose structure and development closely resemble those at mid-latitudes in the atmosphere. As further evidence of the similarity of the dish-pan to the atmosphere, Starr and Long (1953) have demonstrated that eddies in the dish-pan play the same role as eddies in the atmosphere in the maintenance of the angular momentum balance. Measuring velocities at the free surface of a rotating dish-pan experiment, they calculated the angular momentum transports. They found that the average transport was northward at all latitudes with a maximum near the latitude of the maximum westerly "wind", as is the case near the tropopause in the atmosphere.

Secondly, also as in the atmosphere, nearly all of the transport was by means of the eddies.

Thus a dish-pan experiment was conducted with special emphasis on obtaining a long record of the flow in the Rossby regime under conditions as constant as possible. The free surface velocity fields of a subset of this record were measured and statistics of the growth of errors calculated. The following sections describe the experiment itself, the analysis of the data, the computational procedure and our numerical results. In brief, we found a much broader distribution of analogues in the free surface velocity field of the dish-pan than Lorenz (1969) found in the three dimensional atmosphere. The smallest errors encountered doubled initially in 6.6 "days". Applying Lorenz' (1969) hypothesis of quadratic growth of small errors we found that the smallest errors should double in 1.7 "days". Although this value differs from Lorenz' value of 2.5 days for the atmosphere they are not statistically different.

2. PROCEDURE

The first task is to obtain a data-set of measurements of the circulation over an extended number of revolutions in a rotating dish-pan experiment. Lorenz (1969) noted that ideally for two states of the atmosphere to be considered analogues the three-dimensional distributions of wind, pressure, temperature, water vapor and clouds should be similar as well as the geographical distribution of sea-surface temperature, snow cover and so on. Likewise in the dish-pan we should require analogues to have similar distributions of rotation, depth of the working fluid, and heating and cooling rates and their distributions - all of which we can measure and control. In addition the three-dimensional distributions of pressure, fluid velocity, and temperature should be similar. In practice the measurement of all these parameters is impossible. In fact, the only synoptic data which we have is the velocity field obtained from streak photographs of tracers on the surface. Is this in any way representative of the flow through the depth of the pan? Is it representative even of the flow at the upper levels of the fluid? Although a shear stress exists between the fluid and the air above, we also know that the magnitude of this force makes it negligible with respect to the pressure gradient and Coriolis forces. Thus we can say that there is no stress across the upper surface and therefore the velocity field at the surface is representative of the upper layer. Secondly, since in the atmosphere the tropopause similarly acts as a zero-stress boundary, we can identify this layer with the

upper troposphere. Thus the surface flow in the dish-pan can be considered analogously to the 250 mb flow in the atmosphere. In fact under the proper adjustment of the dish-pan parameters, the surface flow exhibits many characteristics of the 250 mb flow in the atmosphere, most notable a strong circumpolar jet. We make this analogy only to draw on our synoptic experience. The 250 mb flow, although characteristic in some sense of the large-scale flow of the atmosphere, contains little information on the smaller scale flow fields below. For example, it tells us nothing about the frontal zones of the lower atmosphere. Likewise the surface flow of the dish-pan does not reveal the frontal zones which have been shown to exist below (Faller, 1956). Therefore, in studying surface flow of the dish-pan we should expect to derive statistics of the large scale circulation only.

Bearing this in mind, two general circulation dish-pan experiments were conducted at the University of Maryland's Institute for Fluid Dynamics and Applied Mathematics. Professor Allan J. Faller directed the experiments and provided streak photographs of the surface. The primary objectives were:

1) To adjust the external parameters to produce a surface flow similar to the 250 mb flow in the atmosphere.

2) To obtain as long a record as possible in the hope of finding good analogues.

As we will see in the description of the experiments, we were unable

to control the character of the flow as might be desired which resulted in a much smaller number of revolutions in the desired flow régime.

Velocity measurements were made from one series of photographs. This turned out to be a difficult process, and further shortened the record which was analyzed. Finally a data-set of approximately one hundred velocity fields was obtained.

A preliminary study had been conducted using a series of 21 photographs (supplied by Professor Faller) of an earlier general circulation experiment. Velocities were measured by hand at eighteen points at mid-radius on the photographs. Westward angular momentum transports were calculated for each case and ranked by size. This statistic provides information on the flow field which is invariant under rotation of the picture. A subjective comparison of the photographs with the closest momentum transports showed a reasonable correlation in the flow fields under the proper rotation. On the other hand, this statistic does not give any measure of the quantitative difference between the flows.

A better criteria for finding analogues was needed. In his study of atmospheric analogues, Lorenz (1969) defined a statistic which was a function of the Root Mean Square difference in the height fields at grid-points averaged over the three pressure levels considered. Height was chosen as the parameter of interest out of expediency. Wind or temperature would have been an equally good choice as they are related to heights geostrophically or hydrostatically on the scales of the grid used. Good analogues were defined as those cases in which

this statistic was small in comparison to its values for two randomly chosen states. In an earlier study (Lorenz 1968) of analogues in the solution of a pair of first-order difference equations, the statistic used was defined as the RMS difference of two successive solutions. We will define our criteria similarly as the RMS difference in velocity fields.

The dish-pan model of the atmosphere is unique in its symmetry. Thus we can compare states not only in a one to one manner as in Lorenz' experiments, but also with a rotation of the frame of reference. If velocities were measured in a polar grid, this could simply be accomplished by calculating the RMS difference while iteratively rotating the field by one grid element. This is not very satisfactory as we should like to rotate the fields arbitrarily for the best correlation between them. Although interpolation between grid points would enable arbitrary rotations, the alternative of writing the velocity filed as an ortho-normal set of functions offers many advantages.

Formally, a variable G which is constant on the circumference of a circle of radius " a " can be expanded in the normalized Fourier-Bessel series (c.f. Lorenz, 1962)

$$G = G_{00} + \sum_{m=1}^{\infty} G_{0m} F_{0m} + \sum_{m,n=1}^{\infty} (G_{nm} F_{nm} + G'_{nm} F'_{nm}) \qquad (2.1)$$

where

$$F_{0m} = J_0^{-1}(j_{1m})\ J_0(j_{1m} r_0) \qquad (2.2)$$

$$F_{nm} = \sqrt{2}\, J_{n-1}^{-1}(j_{nm})\, J_n(j_{nm} r_0) \cos n\varphi \qquad (2.3)$$

$$F'_{nm} = \sqrt{2}\, J_{n-1}^{-1}(j_{nm})\, J_n(j_{nm} r_0) \sin n\varphi \qquad (2.4)$$

Here $r_0 = r/a$, r and φ are polar coordinates, J_n is the Bessel function of order n, and j_{nm} is the mth positive root of the equation $J_n = 0$.

In this case, G is determined by a finite set of velocity measurements. If the series is truncated such that the number of terms is equal to the number of data points, then the series will give an exact representation of the data at the discrete observation points (c.f. Dixon, et al., 1972). However, as we noted, we are concerned with the statistics of the large-scale flow. Secondly, there are errors in the measurements which we would like to filter out. Thus we will truncate the series to a number of terms smaller than the number of discrete data points and solve for the coefficients of the series by minimizing the residual error between the series representation and the data, i.e. by least squares. Furthermore, it is unreasonable to expect to find velocity traces at a set of discrete grid positions. This approach allows us to solve for the coefficients using the actual position of the velocity trace to calculate the Fourier-Bessel functions. Finally it significantly reduces the statistical analysis.

If G denotes one velocity field, $G^{\dagger}$ a different field and and $\overline{(\ )}$ implies an average over the entire field than the squared difference between them,

$$\overline{(G-G^{\dagger})^2} = (G_{00}-G^{\dagger}_{00})^2 + \sum_{m=1}^{M}(G_{0m}-G^{\dagger}_{0m})^2 + \sum_{m,n=1}^{M,N}(G_{mn}-G^{\dagger}_{mn})^2 + \sum_{m,n=1}^{M,N}(G'_{mn}-G'^{\dagger}_{mn})^2. \tag{2.5}$$

In actuality we are dealing with a vector field. We may represent the vector velocity as a complex number

$$\xi = U + iV$$

where U and V are scalar fields written as Fourier-Bessel series as in (2.1). We will define the mean squared difference of two velocity fields $\xi_k = U_k + iV_k$ and $\xi_l = U_l + iV_l$ as mean of the difference of the fields times its complex complement. That is, the mean squared difference

$$D^2_{kl} = \overline{(\xi_k-\xi_l)(\xi_k-\xi_l)^*} = \overline{(U_k-U_l)^2} + \overline{(V_k-V_l)^2} \tag{2.6}$$

where $(\ )^*$ implies complex conjugate. Therefore, the mean squared difference of the vector fields is equal to the sum of the mean squared differences of the scalar fields. Thus we can continue our analysis considering only scalar quantities.

Let us consider the effect of rotating the frame of reference of

one photograph with respect to another. Substituting $\varphi = \theta - \delta$ where δ is a constant angle of rotation into (2.3) and applying a trigonometric identity and (2.4)

$$F_{nm}(r_0, \theta-\delta) = \sqrt{2}\, J_{n-1}^{-1}(j_{nm})\, J_n(j_{nm} r_0)\,(\cos n\theta \cos n\delta + \sin n\theta \sin n\delta)$$
$$= \cos n\delta\, F_{nm}(r_0, \theta) + \sin n\delta\, F'_{nm}(r_0, \theta). \tag{2.7}$$

Similarly

$$F'_{nm}(r_0, \theta-\delta) = \cos n\delta\, F'_{nm}(r_0, \theta) - \sin n\delta\, F_{nm}(r_0, \theta). \tag{2.8}$$

Therefore, substituting into (2.1)

$$G(r_0, \theta-\delta) = G_{00} + \sum_{m=1}^{M} G_{0m} F_{0m}$$
$$+ \sum_{n,m=1}^{M,N} (G_{nm} \cos n\delta + G'_{nm} \sin n\delta)\, F_{nm}(r_0, \theta)$$
$$+ \sum_{n,m=1}^{M,N} (G'_{nm} \cos n\delta - G_{nm} \sin n\delta)\, F'_{nm}(r_0, \theta). \tag{2.9}$$

Rewriting (2.5)

$$\overline{(G(\theta) - G^{\dagger}(\theta-\delta))^2} = (G_{00} - G_{00}^{\dagger})^2 + \sum_{m=1}^{M} (G_{0m} - G_{0m}^{\dagger})^2$$
$$+ \sum_{n,m=1}^{M,N} (G_{nm} - G_{nm}^{\dagger} \cos n\delta - G_{nm}^{\prime\dagger} \sin n\delta)^2$$
$$+ \sum_{n,m=1}^{M,N} (G'_{nm} + G_{nm}^{\dagger} \sin n\delta - G_{nm}^{\prime\dagger} \cos n\delta)^2 \tag{2.10}$$

If we minimize this with respect to δ we find:

$$\sum_{m,n=1}^{M,N} \{ (G_{mn} G^{+}_{mn} + G'_{mn} G'^{+}_{mn}) \sin n\delta + (G'_{mn} G^{+}_{mn} - G_{mn} G'^{+}_{mn}) \cos n\delta \} = 0. \quad (2.11)$$

This can be rewritten

$$\sum_{m,n=1}^{M,N} \Gamma_{m,n} \sin (n\delta_{mn} + \zeta_{mn}) = 0 \quad (2.11a)$$

where

$$\Gamma^2_{mn} = G^2_{mn} G^{+2}_{mn} + G'^2_{mn} G'^{+2}_{mn} + G^2_{mn} G'^{+2}_{mn} + G'^2_{mn} G'^{+2}_{mn} \quad (2.11b)$$

$$\tan \zeta_{mn} = \frac{G'_{mn} G^{+}_{mn} - G_{mn} G'^{+}_{mn}}{G_{mn} G^{+}_{mn} + G'_{mn} G'^{+}_{mn}} \quad (2.11c)$$

If Γ_{mn} is non-zero, then

$$\delta_{mn} = \frac{k\pi - \zeta_{mn}}{n} \quad (2.12)$$

Thus we have an equation for the angle of rotation which minimizes the difference between two fields as a function of m and n. For perfect analogues which differ only by rotation of the reference frame, these δ's would all be equal. However when this is not the case, we would expect different δ's for each m and n. The particular value of δ used was that which minimized the combination of m and

n for which the quantity $(G_{nm} - G^{+}_{nm})^2 + (G'_{nm} - G'^{+}_{nm})^2$ was a maximum. Empirical analysis showed the best results to occur when this algorithm was applied to the zonal velocity component.

Having defined an angle of rotation for two fields, k and l, we then calculate $D^2_{kl}(\delta_{kl})$ by (2.6). Following Lorenz (1969) we define

$$E_{kl} = c/2\,(\log D^2_{kl} - \log \overline{D^2}) \qquad (2.13)$$

where $\overline{D^2}$ is the average of D^2_{kl} over all k and l considered. The constant c = 16/log 2, such that an increase of E_{kl} by 16 units represents an increase in D_{kl} by a factor of 2. We also define an average root-mean square velocity difference X_{kl} by letting

$$E_{kl} = c \log X_{kl} \qquad (2.14)$$

Note that for randomly chosen states $E_{kl} = 0$ and $X_{kl} = 1$.

We will exclude from consideration those states which are less than or equal to 20 rotations apart to exclude possible analogues which are close together in time.

3. THE DISH-PAN EXPERIMENTS

The dish-pan experiments were conducted at the Institute of Fluid Dynamics at the University of Maryland by Professor A. J. Faller and his staff. This particular facility was selected since the dish-pan apparatus is being developed for use as a long term general circulation model. It was hoped that this would permit long records, increasing the possibility of finding good analogues. The first experiment, hereafter referred to as GC-11, was started at 11:15 on 2 February 1971 and ran continuously for 1,533 revolutions (almost 51 hours). During this time the circulation failed to reach a steady-state condition, i.e. a condition of constant heat flux between the hot and cold baths. Modifications were made on the bath controls and a second experiment, hereafter referred to as GC-12, was conducted beginning at 18:00 on 30 March 1971. This ran successfully for 2,504 revolutions (68 hours) before being terminated because of difficulties with the camera system.

3.1 Experimental Set-Up

A schematic representation of the dish-pan and support equipment is shown in Fig. I. The pan is one meter in radius and was filled with water to a depth of 10 cm. A glass cover prevents excessive evaporation and the accumulation of dust on the working fluid. Heating and cooling is by means of water circulated under the lower surfaces of the pan. The cold bath is maintained at a constant temperature by pumping water from a temperature controlled reservoir through the bath. Warm water

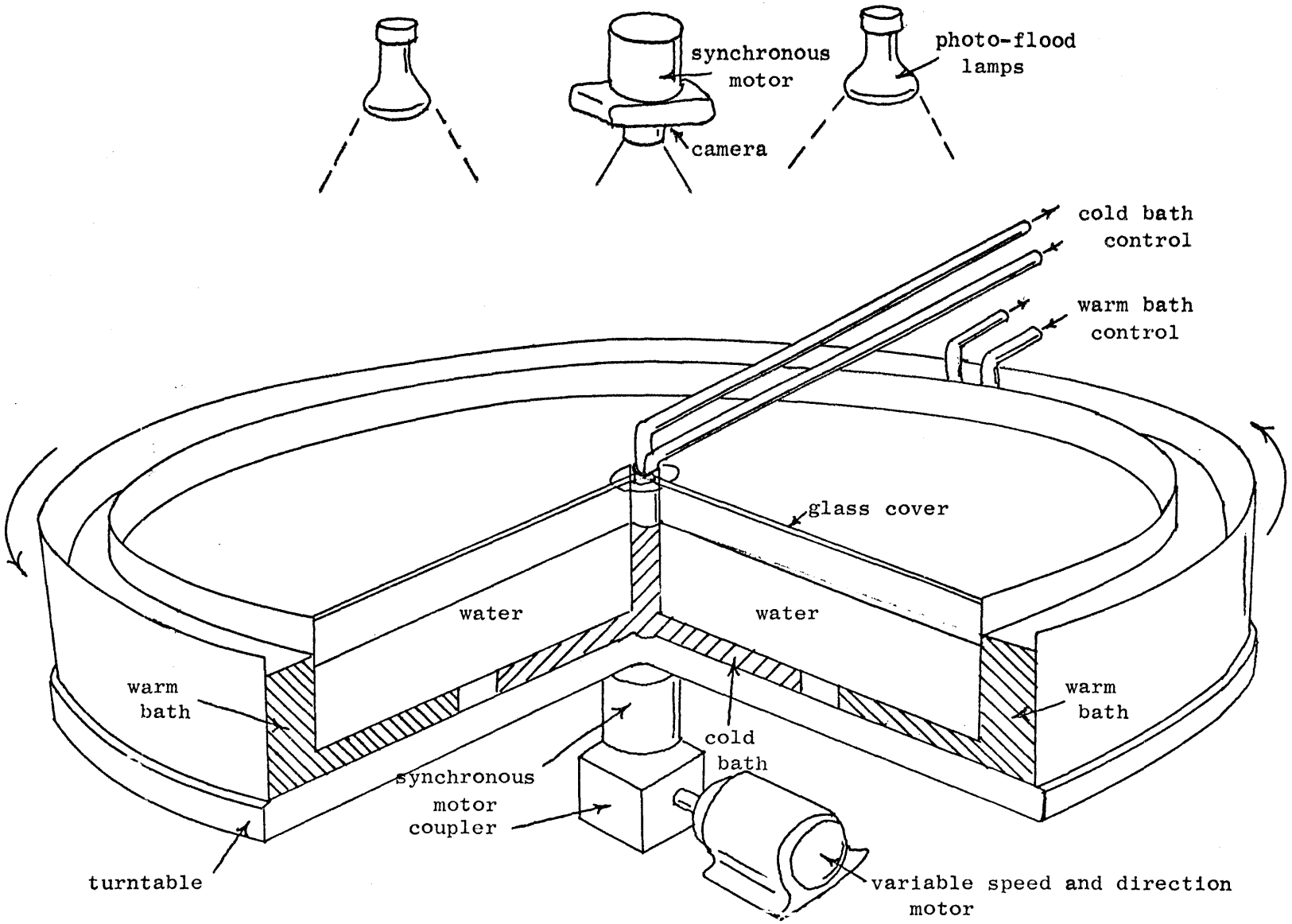

Fig. I. Schematic drawing of the dish-pan apparatus showing the location of the warm and cold baths, the warm and cold bath circulation pipes, the rotating equipment below, and the recording camera above.

is circulated through the warm bath in a closed system. The circulating water is heated at a constant rate. The resultant circulation in the pan will eventually reach an equilibrium condition in which a constant heat flux is maintained between the two baths. The entire pan is rotated on a turntable driven by a variable speed and direction motor. A synchronous motor linked to the turntable drives a similar synchronous motor mounted above the center of the pan, which rotates a camera for recording the surface flow. The camera is a 35 mm SLR with auxilliary film holder and electric drive. This allows up to 250 exposures to be taken between film changes. Lighting is provided by banks of fluorescent lights and also photo-flood lights described in the next section. Also mounted above the pan are infrared heaters to control condensation on the cover glass. Fig. II shows the dish-pan in operation with the cover glass removed. The positions of the warm and cold bath circulation pipes are shown.

3.2 Data Recording

Streak photographs were taken of tracers on the surface in order to measure the velocities from the displacements. The working fluid (water) was dyed a dark purple using permanganate crystals. In the first experiment the tracers were plastic cylinders approximately 3 cm long which were weighted to float vertically in the water. Two problems arose with these during the experiment which led to their replacement. The first was that bubbles would adhere to them causing them to float semi-horizontally. Secondly, surface tension effects made them tend

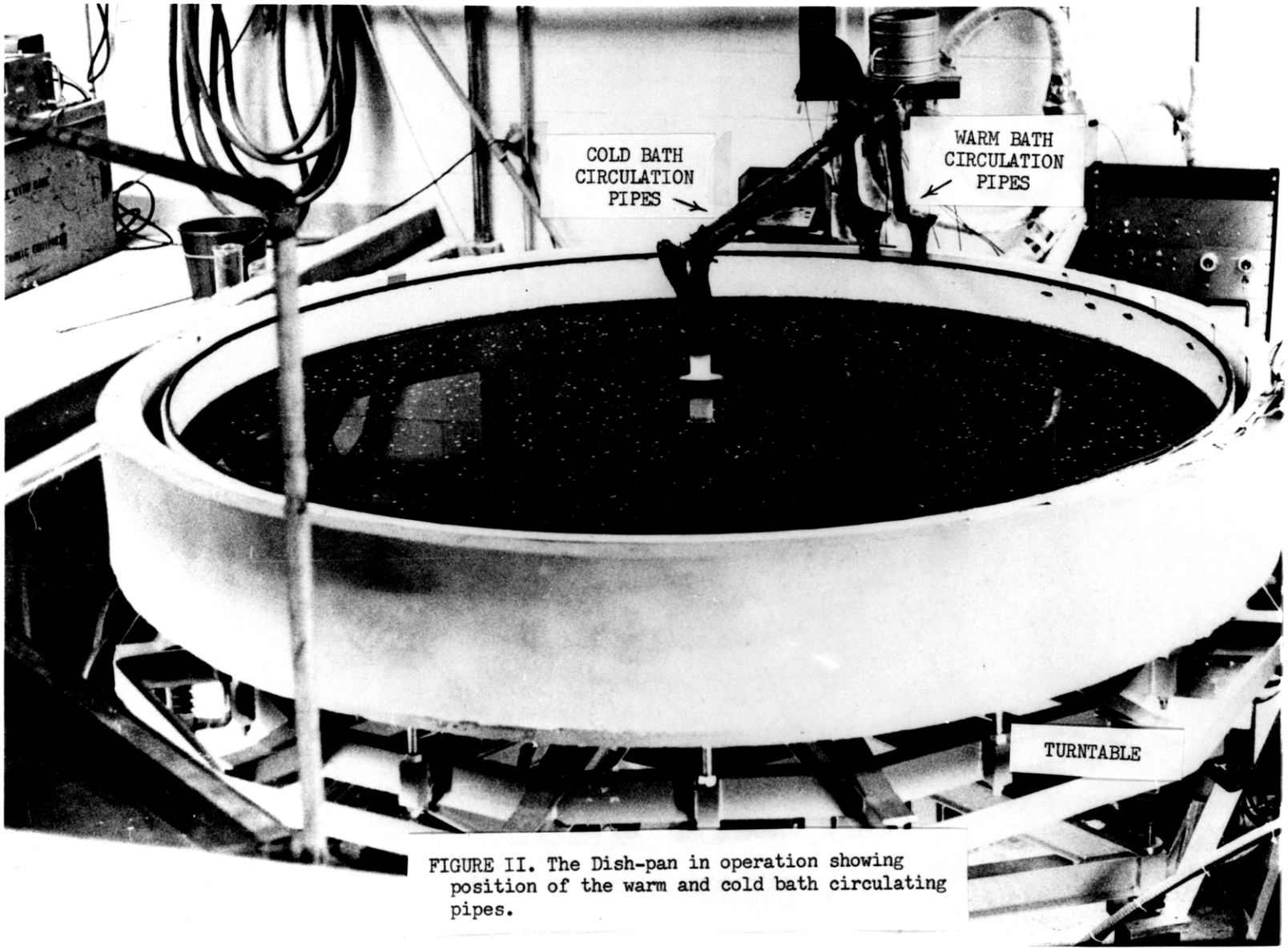

FIGURE II. The Dish-pan in operation showing position of the warm and cold bath circulating pipes.

to stick together leading to a poor distribution of tracers. Thus these tracers were replaced by paper dots. The dots were wetted so that they floated immediately below the surface layer. The only problem encountered was their tendency to absorb water after several hours and sink. Thus more tracers were added at regular intervals.

The pan was photographed once per revolution by the camera rotating synchronously overhead on the axis of rotation. The fluorescent tubes illuminated the surface of the pan continuously. As the pan rotated, it tripped a switch opening the shutter of the camera. After a short delay the photo-flood lights were flashed. After another delay the photo-flood lights were again flashed and the shutter closed. The net effect is to produce a streak with two dots imposed. The dots allow accurate measurement of the displacement of the tracer. The streak's tail allows unambiguous determination of the direction of motion. Fig. III is an example of the photographs with the measuring grid superposed. The two pipes carrying water to the cold bath are seen in the lower right quadrant. Although it appears that they obscure a portion of the tracers, it is possible by careful analysis to retrieve most of the information in this area.

In addition, measurements were made of the parameters of the heat flux in the model. These were automatically recorded on magnetic tape as well as being manually measured and recorded every 30 minutes.

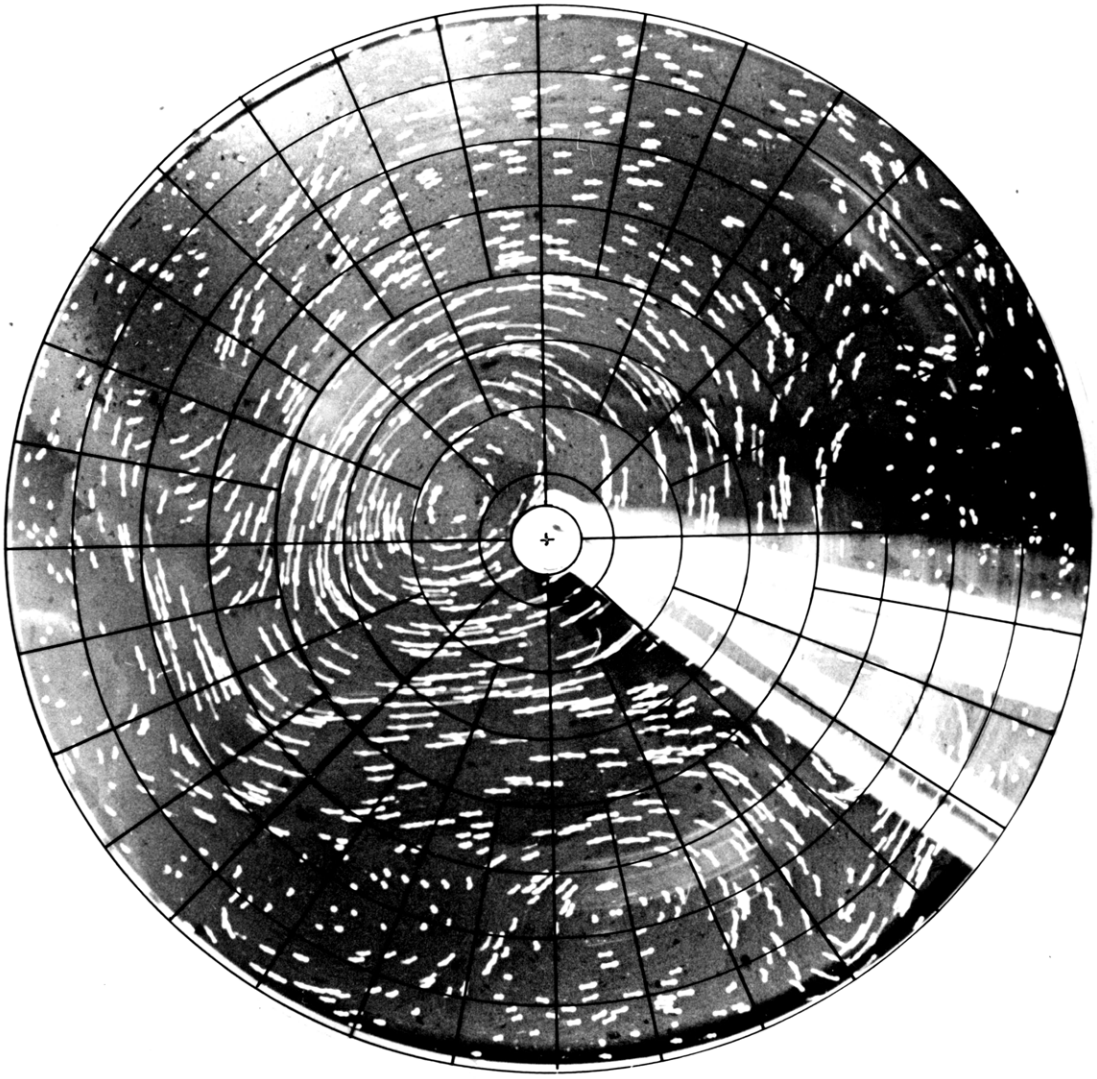

FIGURE III. Streak photograph of the surface tracers with the measurement grid superimposed for revolution 863 of experiment GC-11.

3.3 The First Experiment (GC-11)

The first attempt at obtaining a long term record of the flow in the dish-pan was begun on 2 February 1971. The experiment was run without the glass cover plate in order to keep the plastic tracers separate and free of bubbles. The infrared heaters were used to warm the surface slightly. The room was kept closed in the hopes that an evaporative equilibrium condition would be reached at the surface of the working fluid. The pan was rotated with a relatively uniform period of 120 seconds per revolution. There was a 0.5% increase in the rotation rate during the experiment. The heating of the warm source was adjusted to produce the desired circulation regime.

Lorenz (1967) says that the Taylor number, T_a, and the thermal Rossby, R_{oT}, seem to be the most important dimensionless parameters in determining the flow regime.

The Taylor number is defined as

$$T_a = 4 \Omega^2 h^4 \nu^{-2} \tag{3.1}$$

where Ω is angular velocity of the dish-pan, h the depth of the fluid and ν the kinematic viscosity. It is equal to the square of the ratio of Coriolis to viscous forces.

The thermal Rossby number is defined as

$$R_{oT} = \tfrac{1}{2} g \varepsilon h \Omega^{-2} a^{-2} \Delta T \tag{3.2}$$

where g is the acceleration of gravity, ε the coefficient of

thermal expansion, a the radius of the pan, and ΔT the rim to center temperature difference averaged over the depth of the fluid. As Lorenz notes, the thermal Rossby number is defined to reduce to the familiar Rossby number if the thermal wind relation is valid and the flow near the bottom of the fluid is negligibly small.

As we noted before, in this experiment, GC-11, the character of the flow field was altered by changing the heating of the warm bath. Significant changes also occurred in some of the other important parameters, for example, in the depth of the fluid. In addition there were changes in the kinematic viscosity and the coefficient of thermal expansion because of changes in the temperature of the working fluid, and the increase in the rotation rate. Fig. IV is a plot of R_{oT} and T_a as a function of the revolutions. In as much as these values were calculated from the externally measured temperatures of the warm and cold bath and not those of the fluid itself, only the relative magnitudes of these parameters should be considered and not their absolute values.

In the plot of T_a we see the dominant influence of the decrease in depth of the working fluid. Water was lost by evaporation during the entire experiment at approximately 850 ml per hour. Starting with revolution 750, small amounts of water at the temperature of the warm bath were slowly added at the rim at regular intervals. This stabilized the depth of the working fluid leading to a slight increase in T_a reflecting the increase in Ω . The plot of R_{oT} is a little more complex. It is dominated by the ΔT term. While the cold bath

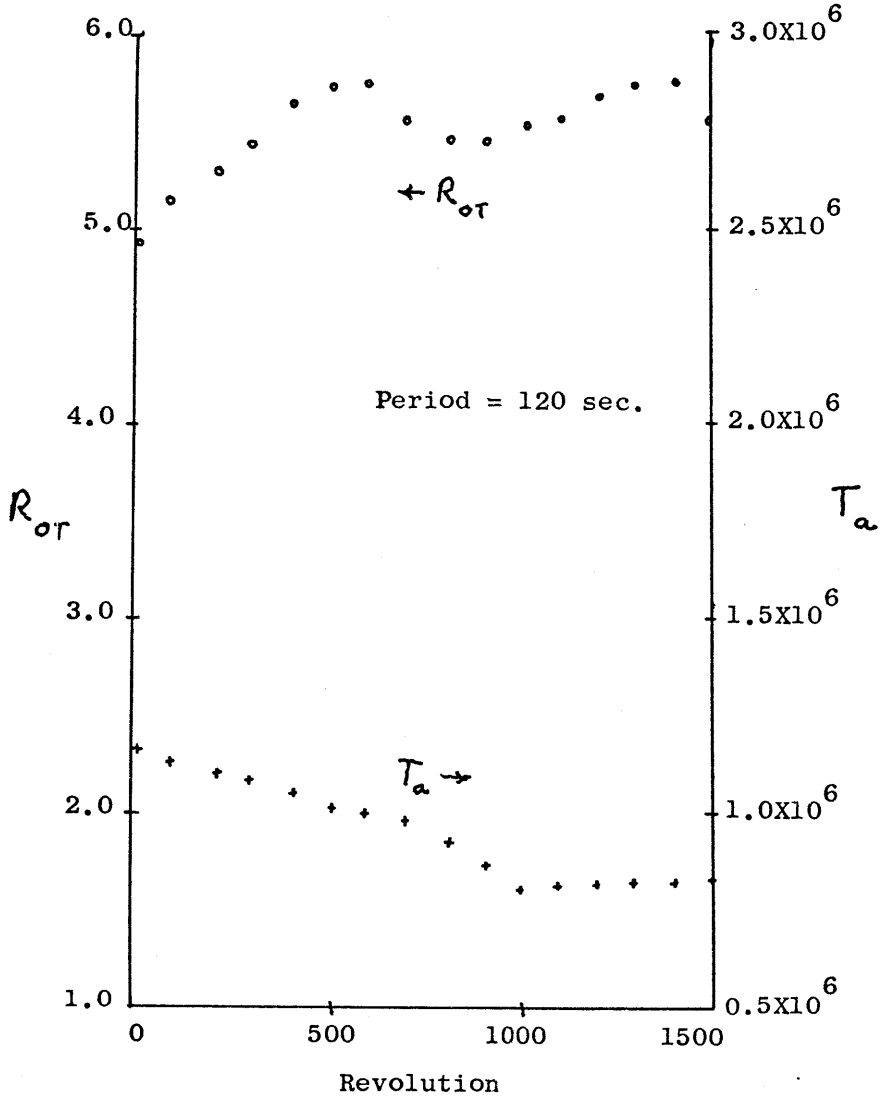

Fig. IV. Plot of the thermal Rossby number, R_{oT}, and the Taylor number, T_a, against the revolution number for experiment GC-11.

temperature was kept nearly constant, the temperature of the warm bath increased until revolution 500 at which point it stabilized for approximately the next 400 revolutions. This behavior is clearly seen in the plot. The region from revolution 600 to 900 is again dominated by the decrease in the depth of the fluid. From this point on, the temperature of the warm bath continued to increase until it again stabilized during the last 100 revolutions. This is also seen in the behavior of R_{or}.

During the entire experiment the flow was in the so-called Rossby regime. The heating was adjusted to produce the desired surface flow characteristics, i.e. subjectively similar to the 250 mb flow of the atmosphere. Initially the surface flow was dominated by three closed cyclonic circulations. As the temperature difference increased this gave way to two and finally one closed center. This was judged to be the closest to atmospheric as it exhibited a "circumpolar" jet with smaller wavelength perturbations superposed. This is the flow shown in Fig. III.

The experiment was finally termined because of dust accumulating on the surface of the working fluid. This produced a film which retarded the surface flow. Such a retarding force produces an Ekman layer in the upper layer making the velocities measured from the tracers unrepresentative. Nevertheless, before this problem became significant, a series of usable photographs of the desired flow type were obtained starting at revolution 867 and continuing through revolution 1109. As seen in Fig. IV, this series was characterized by relatively stable values of R_{or}.

3.4 Second Experiment, GC-12

The short record deemed usable from GC-11 did not seem sufficient for any reasonable analogue search. Therefore a second experiment was attempted. In this case, a glass cover plate protected the surface of the fluid from settling dust. This experiment was very successful in maintaining the desired flow type over long periods. Improvements had been made in the warm bath control system by Professor Faller and his staff so that a relatively constant temperature difference could be maintained. The bath temperatures were set to the values which were found to produce the desired flow field in GC-12 and adjustments of the flow type were made by varying the rotation rate. A plot of R_{oT} and T_a is given in Fig. V. The initial values of these parameters is seen to be close to those in GC-11.

However, the flow at the surface was characteristic of the "Hadley" regime that is, the surface flow was highly symmetric showing westerlies everywhere with no perturbing flows superposed. The difference between the two experiments can only be attributed to the presence of the glass cover, as all the other parameters were essentially unchanged. Note that without the glass cover there was a significant loss of water in the pan through evaporation. A simple calculation shows the evaporative cooling to be of the order of one half the heating of the warm bath. Cooling the upper surface would decrease the static stability of the working fluid. Low static stabilities are conducive to convection and, more importantly, to baroclinic instability.

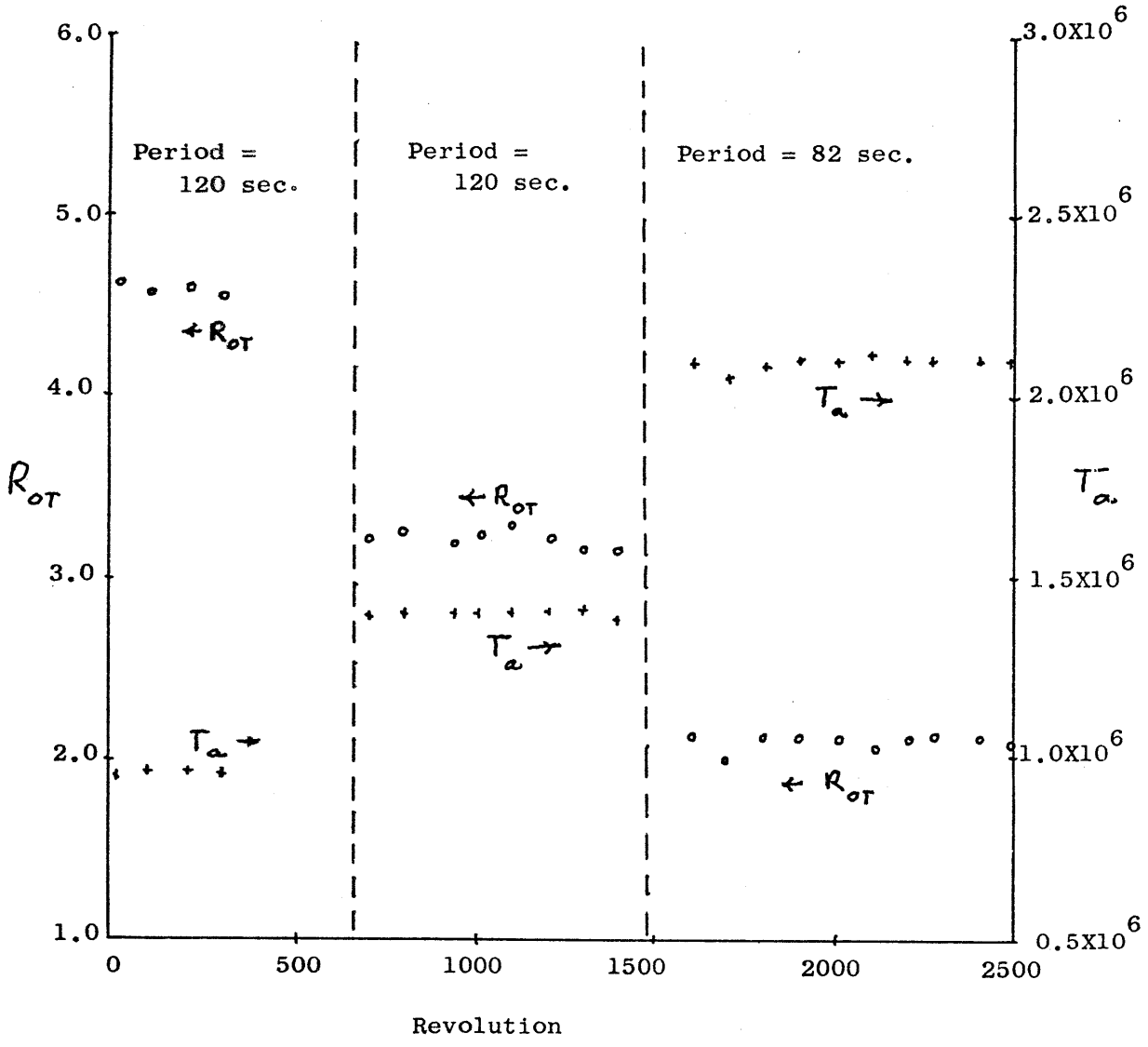

Fig. V. Plot of the thermal Rossby number, R_{oT}, and the Taylor number, T_a, against the revolution number for experiment GC-12. Period of rotation as indicated.

By covering the pan and retarding the evaporative cooling of the surface, the static and baroclinic stabilities were increased. Therefore the stabile circulation found in GC-12 is not surprising.

In this experiment, the character of the flow was modified by changing the rotation rate, as this parameter is easier to control than the temperature difference and produces a faster response. The change in R_{OT} and T_a is seen in Fig. V. During revolution 688, the period of rotation was changed from approximately 120 seconds to 100 seconds. The flow remained essentially symmetric with only small perturbations superposed on the westerly flow. A slightly less stable pattern was desired so that at revolution 1,474 the period was decreased again to approximately 82 seconds. The flow produced was dominated by wave number 3 in the jet, although there were not any significant closed circulations. Although this seemed to be a good analogue to the real atmosphere and this circulation pattern was maintained for over one thousand revolutions, it was not possible to obtain a photographic record of any significant length. Starting around revolution 800, problems began to develop in the film advance mechanism such that successive pictures occasionally overlapped. By revolution 1800 a majority of the photographs were unusuable because of this overlapping. At revolution 2500 the experiment was terminated although the desired circulation was still present because of the problems in the camera system.

4. DATA ANALYSIS

The tracer displacements were measured using an X-Y digital convertor. The streak photographs were projected onto the grid shown in Fig. III. The grid was merely intended as a guide to insure an even distribution of velocity measurements. Thus the grid spaces are only relatively of the same areas, and the tracers measured were those judged most representative of the grid space. There are 172 grid spaces. In the sample considered there were an average 163 velocity measurements per photograph.

The position of the beginning and end point was located manually for each tracer streak. The Cartesian coordinates of these positions were automatically punched onto paper tape. In certain test cases in which a relatively small number of photographs were considered, these paper tapes were converted into cards for input into the MIT IBM 370/155 computer. However, when large amounts of data had to be analyzed, as in the sample considered, the paper tape data was read by highspeed reader and recorded directly onto magnetic tape by means of a Mohawk 6405 computer. In the case of the paper tape to card conversion a control board was wired to translate from paper tape coding to EBCDIC on the IBM 46 Tape-To-Card Punch. The Mohawk computer however wrote the paper tape code onto the magnetic tape without conversion. In addition, there were errors in the data from erroneous measurements, mispunching of the paper tape and erroneous readings by the Mohawk system. Thus a PL/1 program was written to:

1. Translate the data from the paper tape code to the standard EBCDIC for use on the IBM 370/155 computer.

2. Recognize the various data fields. Specifically to recognize a change in photographs, the initialization procedure and the beginning and end positions for each data point.

3. Recognize punching and reading errors.

4. Filter out all data with such errors.

5. Calculate the mid-point of the streak, the zonal and meridional velocity at each data point, and sort and store these according to their position in the grid.

6. Check the consistency of the data for each photograph and between succeeding photographs.

Thus a data set was created containing the velocities and their positions filtered of the errors in reading and data handling. The measurement error still remained.

This error was estimated in two ways. In order to determine the error in the velocities directly, the velocity field of one photograph (revolution 891) was measured ten times. This data was processed exactly as the sample data except that the means and variances for each grid space were calculated. This calculation showed a standard deviation in the velocity measurements over the entire field of $\pm$ 0.00507 in non-dimensional units, with a non-dimensional average speed of 0.02357. We have non-dimensionalized the length by the radius of the pan and time

by the time between flashes of the photo-lights producing the dots on the streak. Thus we have an error on the order of twenty per cent in the velocity measurements. The source of this large error was investigated. The position of an individual spot could be measured within $\pm$ 0.00074 if located carefully. In dimensional units this corresponds to $\pm$ 0.15 mm. Careful velocity measurements were accurate to $\pm$ 0.00134. This is an error on the order of five percent in the velocity, explaining approximately one quarter of the actual error in the velocities. The remainder presumably results from the failure to position the pointer on the X-Y convertor precisely enough. Note that the average photograph required the measurement of three hundred thirty positions. Working at a comfortable rate it required approximately thirty minutes to analyze one photograph, or five and one half seconds to locate and recor each position. More precise positioning would have increased the number of man-hours necessary for analysis significantly. This was judged not to be warranted in this preliminary study.

A Fortran IV program was written to fit the measured velocities to a truncated Fourier-Bessel series. In order to determine the number of zonal and meridional components which were necessary for an adequate fit, a set of experiments was conducted to calculate the Fourier-Bessel coefficients for one velocity field (again revolution 891) truncating the series at various levels for Fourier-Bessel functions calculated at the measured data points and also for functions calculated at the centroid of the appropriate grid element. The series representations were compared by the correlation between the measured data and that calculated from the series representation and also the amount of

computer time required to produce the coefficients of the series. The first conclusion reached was that the use of the grid centroid as the position in the Fourier-Bessel function calculation produced only a 3-5% reduction in the correlation while significantly reducing the amount of computer time required. Thus it was decided to assign each measured velocity to the center of the grid element in which it was found. Recall that one reason for choosing the least-squares fit method was that the actual mid-point of the tracer streak could be used in the calculations as the position of the velocity measurement. In a more precise study this is still a desirable goal. However, the difference in the correlations is small. This is partially due to the fact that the streaks chosen were in most cases those nearest the centroid. The size of the measurement error implies that the accuracy gained by calculating the Fourier-Bessel functions for each data point is not warranted.

In addition, it was also possible to determine the most efficient number of meridional and zonal components in the series. The grid used has eight elements in the radial direction and varies between four elements in the innermost circle to thirty-two in the outer circles in the zonal direction as seen in Fig. III. To avoid aliasing in the coefficients in a Fourier analysis the maximum wave number must not be more than half the minimum number of elements. Applying this rule of thumb requires no more than wave number four in the radial direction. In the zonal direction, we should expand to no more than wave number two, in

as much as there are only four zonal elements near the center of the pan. However, the major circulations occur at mid-radius where the minimum number of zonal elements is sixteen, this implies an expansion to wave-number eight. The experiment conducted to evaluate the effect of truncating the series at various levels confirmed this hypothesis. The correlation between the fitted and measured velocity fields increased up to the case of four radial and eight zonal components, with correlations of 0.944 for the zonal velocity and 0.930 for the radial. Beyond this there was only a small increase in correlation with the number of elements in the series and a significant increase in computing time.

5. RESULTS

Let us consider first the distribution of the values of E_{kl}. For convenience they were classed by truncating E_{kl} to a digit. In addition a character was assigned to each of these classes. Table 1 shows the number of occurrences of each class, its associated character and the number of occurrences N_α in that class for the case of comparison without rotation. We can compare this with Lorenz (1969) by means of the frequency distributions in Fig. VI (a & b). The most striking difference is the spread of the current data with respect to that from the atmosphere. While Lorenz' sample has a standard deviation of 2.11, the data for the dish-pan has a much larger standard deviation of 5.46. In part, we would expect the twenty per cent measurement error to produce a wider distribution. But it also appears that by considering only the free surface velocity field of the model, or analogously only the 250 mb level of the atmosphere, we have significantly increased the possibilities of finding good analogues.

Upon applying the rotation algorithm and computing new values of E_{kl}, we obtain the frequency distribution shown in Fig. VIc. The number distribution of pairs in each class is also given in Table 1. Comparing this with the distribution with no rotation, we see that the net effect has been to shift the distribution towards lower values of E_{kl} as expected. We have also decreased the number of extreme values of E_{kl}. Thus we have changed a portion of the average analogues to fair analogues as we had desired. However, instead of also producing more good analogues, we had likewise changed a portion

TABLE 1. Number of occurrences N_α of each observed value α of $E_{s\ell}$ for straight comparison, N_α, and comparison with rotation, $N_\alpha(\delta)$. Characters used to represent each value in printed output are included.

α	character	N_α	$N_\alpha(\delta)$
-19	1	0	0
-18	2	1	0
-17	3	0	1
-16	4	0	1
-15	5	2	2
-14	6	4	4
-13	7	14	4
-12	8	11	9
-11	9	16	24
-10	A	41	40
-9	B	59	61
-8	C	80	102
-7	D	94	117
-6	E	131	143
-5	F	152	184
-4	G	177	221
-3	H	196	212
-2	J	198	214
-1	K	215	175
0	L	344	329
1	M	158	139
2	N	134	125
3	P	92	94
4	Q	96	96
5	R	76	99
6	S	79	79
7	T	72	74
8	U	60	51
9	V	61	30
10	W	44	23
11	X	35	11
12	Y	20	5
13	Z	7	5
14	*	2	2
15	?	2	0
16	¬	0	0
17	$	0	3
18	&	0	2
19	+	0	3

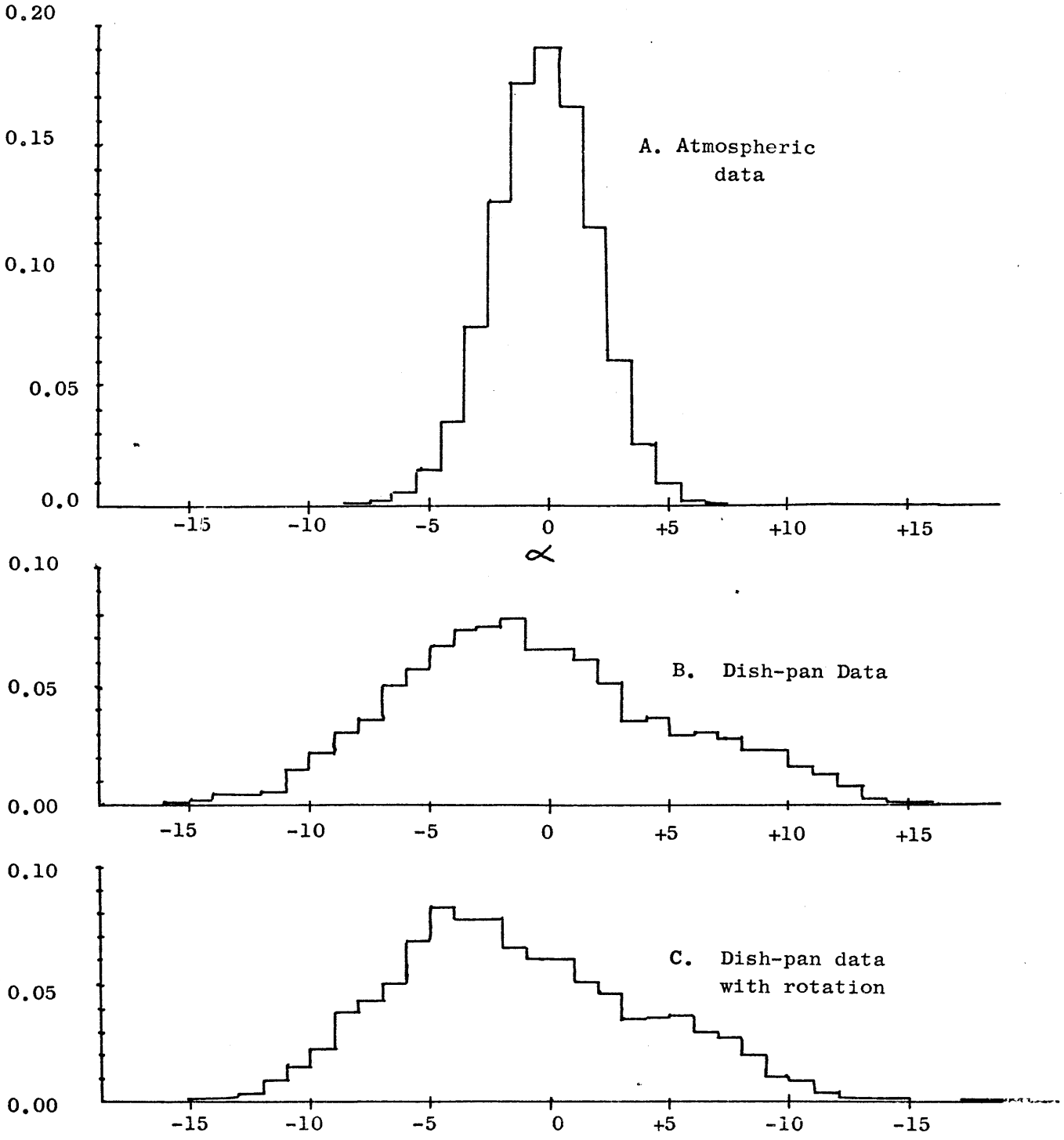

Fig. VI. Frequency distribution of the number of occurrences, N_α, against α, for a) Lorenz atmospheric data, b) dish-pan data without rotation of the frame of reference, and c) dish-pan data with rotation of the frame of reference between pairs of states.

of the good analogues to fair.

Although it is not possible to definitely state the reason for this result, we can make several hypotheses. We can argue that the rotation algorithm does not generate the correct rotation angle. However, before applying this algorithm to the sample data, this procedure was verified using a set of test data. This data consisted of a series of six velocity field measurements of the same photograph, in which the photograph was rotated by 90 degrees between each measurement of the field. When the rotation algorithm was applied to this data set, it produced the correct angle of rotation with an error of $\pm$ 10.2 degrees. This was considered to be reasonable in light of the measurement errors. The other possibility is that the dish-pan was not symmetric as assumed. Standing waves in the flow, set up by topography of the pan could produce such an asymmetry. This effect however, is thought to be insignificant in this experiment because of the care in construction of the dish-pan apparatus. Of more concern is the symmetry of the heating of the lower surface of the pan. As we noted before, this heating was applied by circulating warm water underneath the outer radii and outer walls of the pan. During the second experiment it was noted that the temperature of the warm bath near the bottom of the bath varied by as much as 5 degrees centigrade around the circumference of the pan. It was suggested that this variation might result from air bubbles trapped in the warm bath under the pan. If this were the case, it would lead to significant stationary asymmetries in the heating of the working fluid. The effect would be to generate standing waves in the flow similar to the standing

waves produced in the atmosphere by the asymmetric heating of land and water. In order to evaluate the magnitude of asymmetric flow, the mean velocity field was calculated for the entire sample. The Fourier coefficients of the average velocity field were calculated at mid-radius. The zonal component of the velocity showed a strong wavenumber seven component with the secondary maximum wavenumber one. The meridional component showed a strong wavenumber one component with secondary maxima at wavenumbers three and seven. This seems to indicate some asymmetry in the dish-pan which generates standing perturbations of wavenumbers one and seven. In addition we feel that the errors in the measurement of the velocity field produced errors in the rotation algorithm sufficient to make the results unreliable. The possibility of rotating the reference frame between pairs was not pursued further, and the rest of the analysis was performed with the statistics generated without rotation.

In order to study the growth of errors in the data, we will consider the growth of the values of $E_{k+m,\,l+m}$ for $m = 1,2,\ldots$ In as much as the smallest value of E_{kl} in the sample is -18 with a corresponding X_{kl} of 0.453, that is slightly less than half as large as the difference between randomly chosen states, we will retrieve what information we can from the analogues available. Fig. VII shows a portion of the computer printout of values of E_{kl} represented by the characters given in Table 1. We are concerned with the variation of these values along the diagonals.

Rather than analyse this display in detail, we have calculated $E_{\alpha}(m)$, the average value of $E_{k+m,\,l+m}$ for each category

```
QLLLH=LHHJMPNMJJLNLKLQURQNTKQNNL
SQNNN=KLLMLMQPQPPPNMMRTTSPUMLQNM
RPNLM=LKLLPMMNPMPQNPPUUQQSTLMNMP
================================
LHFFF=B7AB8BHHLHGFDHDKNKJHQAFHGE
LGEDH=ABCCE7DFLKHFCLKMNGFKREAEHH
LFECF=BCEEHC99JKJHCHJQSLGFRGGDGH
LF98B=B7BAGHGBCGEHFDALRMLJQCJGGF
LHCCB=96699EHGHFEFEEAJPLLJQAFJGE
KGCBF=B78CA8FEKKGECJGLNKKJRCBHHG
LEDBE=BC8EJEBDJKGHCGHQSMKFRGEFJJ
LGDCD=88BAKLKFBDFHFDENRMLKPEJDDF
LKHHF=DADBBGKKKFFHJKFLQLKJRDKJGE
MKGHJ=ECCGECGJLLJKHLHLQMLLSFGLLK
LHDAH=BBCAFBDAJLJHEKHNQLLKSEEGHJ
MJDDF=DAEBHJHFGJHKGDFMSNNLRCLKKK
LHFED=B977FJJHFEEJFECLRMLKQDKGFF
LKJHH=FCFD8ELLLKKJJKFKPLLLSFKLJH
LHGEJ=GFDGHBCHMLKJGLKPQKJLTKFHLL
LHEDH=CDFBHFFBJLHJEJHNSMLKRFHEHJ
LJGFG=DCFFFFHFJJKLGJJNRLKJQFJEFH
MKJHH=GFGHFFGJLKLLJKJLQLJKSHJGHJ
KJGEH=HGHJJDCDJLLLKLKMQLLLUKKJLL
JGB98=GCEEJKHEAFGKJHFMRNMLTHLLLL
LJEED=DCBCFJKJGFDKJGCLQNMLSGLLKK
LKHHG=ECDUDFKLKGGJKLGJNLLLSGKLKJ
```

Fig. VII. Selected values of E_{kl} corresponding to characters given in Table 1, printed out by computer. An "=" denotes missing data. Successive rows correspond to values of k for revolution number 881 to 906. Successive columns correspond to values of l from 918 to 949.

in which $E_{kl} = \alpha$. Analogously to (2.14) we let

$$E_\alpha(m) = c \log X_\alpha(m). \tag{5.1}$$

The values of $E_\alpha(m)$ for m equal to 0 to 8 are given in Table 2. We notice in general that as m increases $E_\alpha(m)$ approaches zero. Since the number of occurrences in each case decreases with m , the values of $E_\alpha(m)$ for larger values of m vary irratically because of the small sample size.

Lorenz (1969) argues that the growth of an arbitrary error is the superposition of "normal modes". Initially some ot the normal modes will grow quasi-exponentially while others will decay quasi-exponentially. For an error initially of random shape, these growing and decaying modes should tend to cancel when $m = 0$. As m increases the decaying modes become insignificant, and the amplifying modes dominate. When m becomes sufficiently large, $X_\alpha(m)$ approaches 1, the value for randomly chosen states, and the amplification decays because of nonlinear effects.

To study the growth rate of errors once the decaying modes are small, we have plotted in Fig. VIII the values of $X_\alpha(m+1)$ against $X_\alpha(m)$ calculated from the values of $E_\alpha(m)$ in Table 2. Values for $m = 0$ have not been included since the decaying modes are important for those cases. Further those cases in which E_{kl} was less than or equal to -14 have not been included because the number of cases was too small. Also following Lorenz (1969) we have not included values for which $X_\alpha(m) > 0.95$. The distance of the dots above the diagonal indicate the amplification of X_α during one "day".

TABLE 2. Average values $E_{\alpha}(m)$ of $E_{k+m,\,l+m}$ for those instances $E_{kl} = \alpha$.

α	m = 0	m = 1	m = 2	m = 3	m = 4	m = 5	m = 6	m = 7	m = 8
-18	-18.26	-13.58	-12.21	-11.10	ND	ND	ND	ND	ND
-17	ND	ND	ND	ND	ND	ND	ND	ND	ND
-16	ND	ND	ND	ND	ND	ND	ND	ND	ND
-15	-15.67	-9.90	-0.28	-5.24	5.45	6.23	0.13	11.50	8.31
-14	-14.63	-11.57	-4.54	-1.82	-3.54	-3.82	-6.16	1.02	-3.59
-13	-13.46	-11.93	-8.23	-5.49	-2.50	-3.14	-1.02	-3.92	-1.33
-12	-12.55	-9.92	-7.54	-4.40	-2.68	-2.57	-1.62	-1.31	1.06
-11	-11.47	-8.83	-5.85	-4.85	-2.89	-2.35	-2.29	0.28	-0.52
-10	-10.41	-8.45	-6.33	-4.72	-4.30	-2.66	-1.66	-0.90	-1.23
-9	-9.46	-6.93	-5.61	-5.15	-2.77	-2.63	-1.79	-2.05	-0.42
-8	-8.42	-6.36	-3.88	-3.03	-2.27	-2.73	-2.40	-1.37	-0.15
-7	-7.45	-5.47	-2.78	-2.06	-1.22	-2.69	-0.21	-0.54	0.48
-6	-6.47	-3.64	-3.80	-2.87	-0.87	-1.82	-0.56	-0.15	0.54
-5	-5.50	-3.57	-3.71	-3.24	-1.39	-1.30	-0.83	0.03	-0.50
-4	-4.48	-2.58	-2.44	-1.16	-1.39	-0.16	0.31	0.55	0.33
-3	-3.48	-1.60	-2.08	-1.85	-0.04	-0.95	0.31	0.03	-0.32
-2	-2.46	-0.60	-1.27	-0.56	-0.38	0.11	0.48	1.12	1.29
-1	-1.51	-0.32	-0.98	-0.76	0.08	-0.12	0.50	0.88	0.78
0	-0.00	0.96	-0.56	-0.19	-0.50	0.80	-0.33	0.14	0.20
1	1.51	1.72	-0.39	0.69	0.10	0.51	-1.26	-0.39	-0.31
2	2.48	1.82	0.73	0.42	-0.28	0.71	-1.02	-0.46	-1.73
3	3.50	0.22	-0.98	-1.45	-1.66	-0.44	-1.10	-1.19	-1.66
4	4.47	-0.81	0.59	0.39	-0.65	0.69	0.18	-1.88	-1.50
5	5.47	-1.11	0.37	0.15	0.56	1.14	-1.14	-2.52	-0.87
6	6.48	-1.05	0.86	0.95	1.02	-0.09	-0.17	-1.53	-0.27
7	7.49	-1.42	2.12	-0.09	3.05	0.07	-1.20	-0.70	0.62
8	8.47	-0.23	4.17	-0.62	3.05	1.12	-1.20	-0.44	-0.36
9	9.38	-0.09	4.05	-1.53	2.97	1.36	-1.97	1.49	1.04
10	10.46	1.83	4.60	0.58	3.55	2.66	0.48	1.11	1.82
11	11.45	2.63	4.69	2.83	3.44	-0.59	-2.38	-1.65	-3.62
12	12.46	2.17	5.43	5.58	3.94	-1.93	-4.54	-2.66	-2.18
13	13.62	2.28	7.81	-0.70	6.26	6.08	0.54	-0.68	0.86
14	14.49	-2.61	3.18	2.81	ND	ND	ND	ND	ND
15	15.95	5.03	5.45	2.93	ND	ND	ND	ND	ND

* ND = No Data

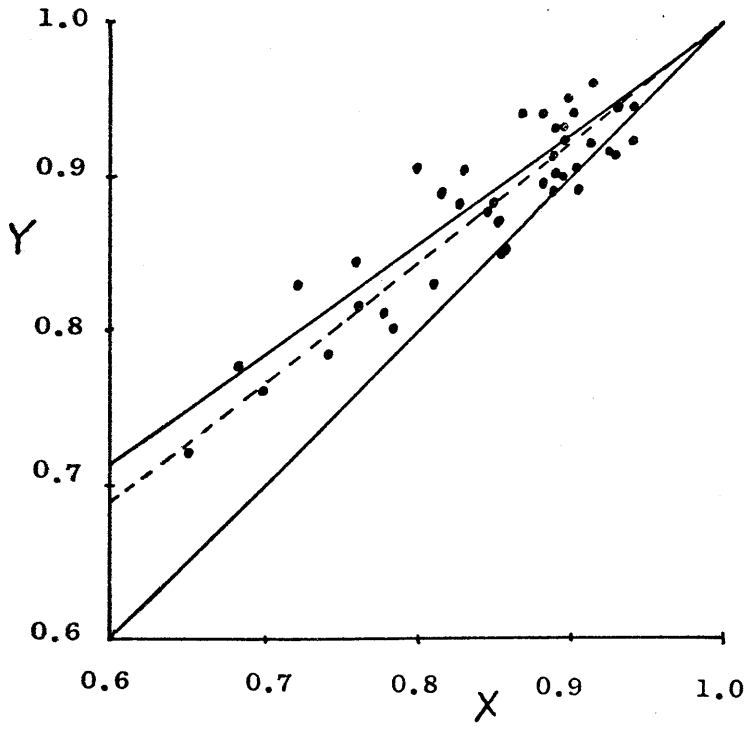

Fig. VIII. Observed values of $Y = X(m+1)$ against $X = X(m)$ for all instances where $E_{tol} > -14$, $m \geq 1$ and $X \leq 0.95$. Line $Y = X$ is included for reference. The dashed line, $Y = 0.78X + 0.22$, is the best fit line to Lorenz' sample of atmospheric data. The upper solid line, $Y = 0.67X + 0.32$, is the least squares regression line for the data presented.

This plot can be compared directly with Lorenz' (1969) plot for the atmosphere. Lorenz' data did not deviate greatly from the dashed straight line shown in Fig. VIII. This line passes through the point (1,1) with a slope of 0.78. A least squares fit of the dish-pan data produces the upper solid line, which also passes through (1,1) but with a slope of 0.666. The deviation of the data points about this line is much greater than Lorenz' data because of the smaller sample size and measuring error. The smaller slope indicates a faster amplification rate for errors.

The left-most point in Fig. VIII corresponds to an amplification rate of 1.11 per revolution. Continued growth at this rate would imply that errors of this magnitude would double in 6.6 revolutions. This value corresponds to an error of .650 times that for randomly chosen states. As we noted before this cannot be considered a small error. However, since Lorenz (1965) has shown that small errors amplify faster than large errors, we may conclude that the typical doubling time for small random errors in our experiment is not greater than 6.6 revolutions (days). In his study of the atmosphere Lorenz found an upper bound of 8 days for the doubling time of small random errors.

In order to obtain specific estimates of the doubling time of small random errors we make use of a quadratic hypothesis of error growth introduced by Lorenz (1969). Our model of the growth of errors calls for the quasi-exponential growth of small errors to cease as the errors become large because of the nonlinear terms in the governing

equations. Lorenz assumes that the principle nonlinearities are the quadratic terms representing the advection of temperature and velocity fields. It then follows that the principle nonlinear terms in the governing equations of the field of errors will also be quadratic. Lorenz then argues that for arbitrary values of α, and for values of $m \geq 1$, the quantity $X_\alpha(m)$ defined by (5.1) is governed by the quadratic equation

$$\frac{dX}{dm} = aX - bX^2 \tag{5.2}$$

Since $X \to 1$ as $m \to \infty$, the constants a and b must be equal. The general solution of (5.2) is then

$$X = (1 + ce^{-am})^{-1} \tag{5.3}$$

Thus for any positive lag

$$X(m+n) = X(m)\left[e^{-an} + (1 - e^{-an})X(m)\right]^{-1} \tag{5.4}$$

The curve of $X(m+n)$ against $X(m)$ is a rectangular hyperbola passing through the point (1,1) with a slope of e^{-an} and through (0,0) with a slope of e^{+an}. The slope of the curve through the origin represents the amplification factor for small errors during days.

For our data we know that the slope of the least-squares regression line through the point (1.1) is 0.666. Assume that the curve of $X(m+n)$ against $X(n)$ for $n = 1$ passes through (1.1)

with approximately the same slope. Then $e^{-a} = 0.666$ which implies $a = 0.406$. The doubling time for small errors, obtained by setting $e^{an} = 2$ is approximately 1.7 revolutions (days). Lorenz' best estimate of the doubling time of small errors in the atmosphere was 2.5 days. We would like to know how well these values correspond?

As we noted earlier, the scatter of points used in determining this value of the amplification rate of errors in the dish-pan was significantly larger than that of Lorenz' atmospheric data because of the smaller sample size. The standard deviation of the least squares regression line for our data was found to be 0.056. The 95% confidence limits on the slope are therefore .554 and .778 corresponding to doubling times of 1.2 and 2.8 revolutions. In particular the slope of Lorenz' fitted data lies within 1.6 standard deviations of our calculated value for the dish-pan. Therefore, we are not justified in saying that there is any statistical difference in the values. This supports our original assumption that the flow in the dish-pan is a good analogue of the flow in the atmosphere.

6. SUMMARY AND CONCLUSIONS

A data set of one hundred measurements of the free surface velocity field of a dish-pan model of the atmosphere was assembled. This data included a relatively large (20%) measurement error. The root-mean-square difference of the velocity fields was calculated as a measure of the difference between two fields for those pairs greater than twenty revolutions apart. This difference was then treated as an error superposed on one of the two states and its subsequent growth was analyzed.

No truly small errors were found although the distribution of the errors showed a much wider distribution then found for the atmosphere by Lorenz. The smallest error encountered indicated small random errors would double in not more than 6.6 revolutions or days. Extrapolating the growth rate for moderate errors back by assuming that the growth of errors is governed by a quadratic relationship, we estimated that truly small random errors would double initially in 1.7 revolutions or days. This may be compared with Lorenz' similarly derived value of 2.5 days for the atmosphere. Because of the smaller sample size and the measurement error, we cannot say that these values are statistically different.

Our value does differ significantly however from the value of 5 days estimated by Charney et al. (1966) based upon numerical general circulation models. But as Lorenz (1969) notes, only the statistics of the small-scale motions influence the larger scales in these models, and at any particular instance these statistical properties are determined by the large-scale motions themselves. Thus the influence of

the small-scales upon the large scales is not adequately modelled. In the current method of analyzing the growth by the study of analogues in the flow, we implicitly have included the influences of these small-scale motions. We would therefore argue that actual value of the initial doubling time of small random errors is on the order of two to three days.

ACKNOWLEDGEMENTS

This study would not have been possible without the assistance of Professor A.J. Faller, Robert Kaylor and Lee Barnhart of the University of Maryland who set up and conducted this dish-pan experiment and provided photographs of the surface tracers as well as much helpful advice. In addition, the author wishes to thank Leslie Mandl and Robert Rebello of the MIT computation Center for their consultation in programming. Also to Professor E.N. Lorenz for his advice and continued patient support of this study, my wife Jan for her understanding and typing of draft copies, and finally to Marie L. Gabbe for her able typing of the final draft.

REFERENCES

Dixon, R., E.A. Spackman, I. Jones, and A. Frank, 1972: The global analysis of meteorological data using orthogonal polynomial base functions. JAS, 29, 609-622.

Charney, J.G., et al., 1966: The feasibility of a global observation and analysis system. Bull. Amer. Meteor. Soc., 47, 200-220.

Faller, A.J., 1956: A demonstration of fronts and frontal waves in atmospheric models. J. Meteor., 13, 1-4.

Flemming, R.J., 1971: On stochastic dynamic prediction, II. Predictability and utility. Monthly Weather Review, 99, 927-938.

Fultz, D., R.R. Long, G.V. Owens, W. Bohan, R. Kaylor, and J. Weil, 1959: Studies of thermal convection in a rotating cylinder with some applications for large-scale atmospheric motions. Meteor. Monographs, Amer. Meteor. Soc., 104 pp.

Leith, C.E., 1971: Atmospheric predictability and two dimensional turbulence. JAS, 28, 145-161.

Lorenz, E.N., 1962: Simplified equations applied to the rotating-basin experiments. JAS, 19, 39-51.

Lorenz, E.N., 1963: Deterministic nonperiodic flow. JAS, 20, 130-141.

Lorenz, E.N., 1967: The nature and theory of the general circulation of the atmosphere, WMO, 161 pp.

Lorenz, E.N., 1968: On the range of atmospheric predictability. Proceedings of the First Statistical Meteorological Conference, AMS, 11-19.

Lorenz, E.N., 1969: Atmospheric predictability as revealed by naturally occurring analogues. JAS, 26, 636-646.

Lorenz, E.N., 1969a: The predictability of a flow which possesses many scales of motion. Tellus, 21, 289-307.

Lorenz, E.N., 1972: Barotropic instability of Rossby wave motion. JAS, 29, 258-264.

Robinson, G.D., 1967: Some current projects for global meteorological observation and experiment. Q. J. Roy. Meteor. Soc., 93, 409-418.

Starr, V.P., and R.R. Long, 1953: The flux of angular momentum in rotating model experiments. Geophys. Res. Paper No. 24, 103-113.

Thompson, P.D., 1957: Uncertainty of initial state as a factor in the predictability of large scale atmospheric flow patterns. Tellus, 9, 275-295.